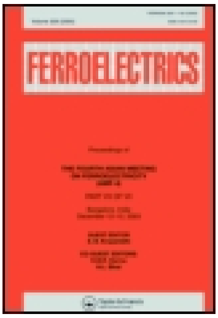

Ferroelectrics
Publication details, including instructions for authors and subscription information:
http://www.tandfonline.com/loi/gfer20

THz Time-Domain Spectroscopic Studies of a Ferroelectric Liquid Crystal in the SmA* and SmC* Phases

Tsung-Ta Tang [a], Ru-Pin Pan [b], Yi-Chao Wang [a] & Ci-Ling Pan [a]

[a] Department of Photonics, Institute of Electro-Optical Engineering

[b] Department of Electrophysics

[c] National Chiao Tung University, Hsinchu, Taiwan, 30010, R.O.C.
Published online: 20 Sep 2010.

Ferroelectrics, 364:72–77, 2008

ISSN: 0015-0193 print / 1563-5112 online
DOI: 10.1080/00150190802049210

THz Time-Domain Spectroscopic Studies of a Ferroelectric Liquid Crystal in the SmA* and SmC* Phases

TSUNG-TA TANG,[1] RU-PIN PAN,[2,*] YI-CHAO WANG,[1]
AND CI-LING PAN[1]

[1]Department of Photonics and Institute of Electro-Optical Engineering
[2]Department of Electrophysics
[3]National Chiao Tung University, Hsinchu, Taiwan 30010, R.O.C.

We report complex refractive indices of a ferroelectric liquid crystal (FLC) ZLI-4654-000 from 0.3 to 3.0 THz by THz time-domain Spectroscopy. Extraordinary and ordinary refractive indices of this FLC in the SmA phase (67.9°C) as well as the SmC* phase (58.1°C) are determined. The birefringence of the FLC varies with frequency but is comparable to its value in the visible, 0.13, while the imaginary indices of refraction in both phases are ≤ 0.06. Absorption bands are found for ordinary waves in both phases and e-waves in SmA* phases.*

Keywords Ferroelectric liquid crystal; smectic; THz; far infrared; time-domain spectroscopy; birefringence; absorption

Introduction

Recently, there have been increasing interests in the study of liquid-crystal-based devices for application in the sub-millimeter wave or THz (1 THz $= 10^{12}$ Hz) frequency range. Several THz photonic devices with nematic-liquid-crystal-enabled functionalities have been demonstrated [1–7]. These include magnetically [1–3] and electrically tuned [4–6] phase shifters with phase shift beyond 360° at 1 THz and a two-element Lyot filter that can be continuously tuned from 0.388 THz to 0.564 THz [7].

With sub-millisecond response time, ferroelectric liquid crystals (FLCs) are widely employed for display and other photonic applications in the visible [8–10]. They are, therefore, also attractive candidates for future THz photonic devices. For these applications, the knowledge of the extraordinary and ordinary refractive indices, n_e and n_o, as well as the birefringence ($\Delta n = n_e - n_o$) of FLCs in the far-infrared (submillimeter wave) or THz frequency range is essential. Employing THz time-domain spectroscopy (THz-TDS) [11], we have shown that the THz (0.2–1.0 THz) birefringence of a well-known nematic LC, 4′-*n*-pentyl-4-cyanobiphenyl (5CB), is in the range of 0.15 to 0.21, while that of 4-(trans -4′-Pentylcyclohexyl)-benzonitrile (PCH5) is from 0.01 to 0.08 at room temperature [12–14]. About the same values of birefringence (∼0.2) were reported in the LC mixture, E7

Received November 5, 2007; in final form November 13, 2007.
*Corresponding author. E-mail: rpchao@mail.nctu.edu.tw

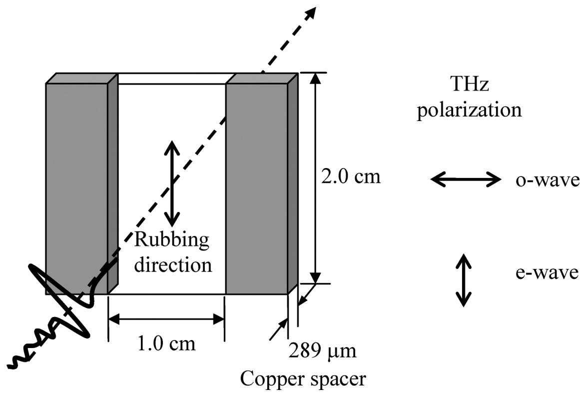

Figure 1. The configuration of the FLC cell and its geometry with respect to the incident terahertz wave. (See Color Plate X)

(by Merck) [15] and a liquid crystal polymer [16]. High-frequency dielectric relaxation of liquid crystals was revealed through a THz time-domain spectroscopic studies of liquid crystal colloids [17]. Strong Terahertz dichroism of MBBA on rubbed substrate was observed [18]. The isotropic liquid, liquid crystal and crystal phases of the bent-core liquid crystal P-8-PIMB were found to be clearly distinguished by their THz spectra [19].

In this work, we employ THz-TDS to determine the refractive indices of a ferroelectric liquid crystal from 0.3 to 3.0 THz, for the first time to our knowledge.

Experimental Methods

The cell was prepared by sandwiching the commercial available FLC, ZLI-4654-000 (Merck) between two fused silica windows. This FLC has a SmC* phase between -10 and 65°C and a SmA* phase between 65 and 69°C. Homogeneous alignment of the FLC was achieved by rubbing the substrates that was coated with polyimide (SE-130B, Nissan). Precision-machined copper pieces, $289 \pm 4\ \mu$m in thickness, were used both as spacers and electrodes for biasing the FLC cell up to 1500 Volts. The cell was mounted in a copper block for which the temperature can be varied and maintained within $\pm$ 0.1°C. The configuration of the cell and its geometry with respect to the incident terahertz wave are shown in Fig. 1.

An antenna-based THz-TDS system with a collimated beam at the sample position [11] had been used. A schematic of the THz-TDS system is shown in Fig. 2. Terahertz pulses, generated by femtosecond-laser-excited dipole-type antenna fabricated on low-temperature-grown GaAs, were collimated by an off-axis parabolic mirror and propagated through the sample at normally incidence. A pair of parallel wire-grid polarizers, before and after the sample, was employed in order to ensure the polarization state of THz wave. The THz fields of extraordinary wave (e-wave) and ordinary wave (o-wave) are parallel and perpendicular to the rubbing direction of FLC cell, respectively. The transmitted THz pulses were focused on another dipole-type antenna gated by time-delayed probe pulses and oriented to detect THz waves polarized parallel to the incident THz wave polarization. The beam size of the THz wave through the sample was about 0.8 cm in diameter. Our THz time-domain spectrometer can be purged with nitrogen and maintained at a relative humidity of $3.0 \pm 0.5\%$.

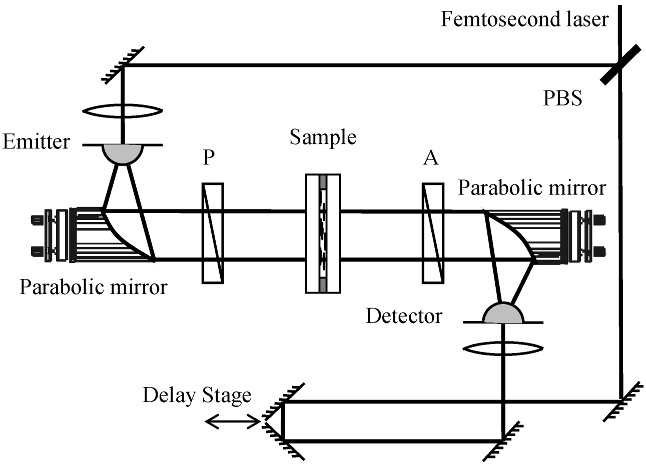

Figure 2. The schematic experimental setup for THz time-domain spectrometer. PBS: Polarizing Beam Splitter; P: polarizer; A: analyzer.

Results and Discussions

The complex optical constants are extracted from the THz-TDS in the usual manner. A brief account can be found from our previous papers [12–15]. Details will be published elsewhere. In Fig. 3, the THz-band real extraordinary and ordinary indices of refraction of the FLC in both the SmA* phase (67.9°C) and the SmC* phase (58.1°C) are shown. In the 0.3 to 3.0 THz range, we determine that n_e varies between 1.54 and 1.59, while n_o varies from 1.44 to 1.52 for the SmA* phase. For the SmC* phase, $n_e = 1.56{\sim}1.64$, and $n_o = 1.44{\sim}1.51$. The birefringence of ZLI-4654-000, $\Delta n = n_e - n_o$, is thus between 0.03 and 0.16, depending on the phase and frequency. In comparison, the birefringence for the FLC in the visible region is reported to be 0.13 at 589 nm, according to the Merck data sheet.

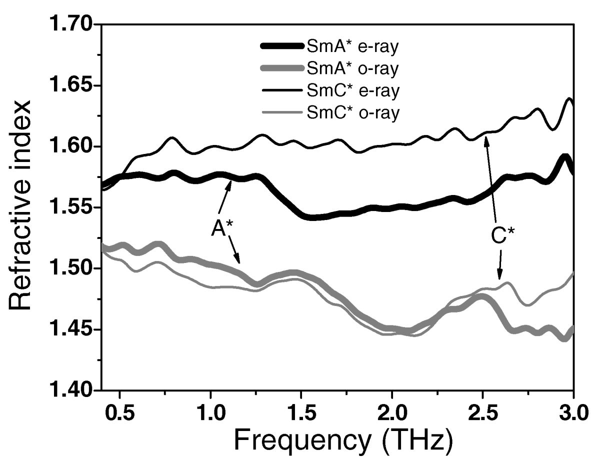

Figure 3. The THz-band real extraordinary and ordinary indices of refraction of the FLC in the SmA* phase (67.9 °C) and SmC* phase (58.1°C).

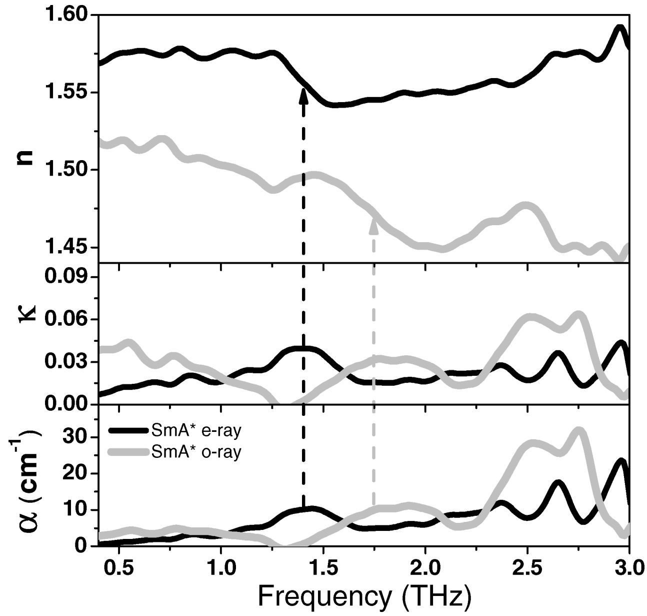

Figure 4. Frequency dependence of the THz-band extraordinary and ordinary absorption coefficients of the FLC in the SmA* phase (67.9°C). To compare, both real and imaginary indices of refraction are also shown. The dashed lines indicate possible positions of the absorption bands.

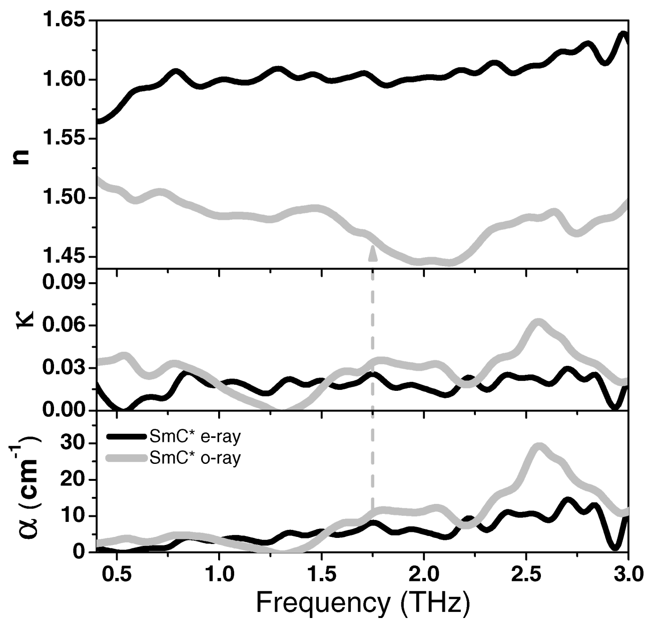

Figure 5. Frequency dependence of the THz-band extraordinary and ordinary absorption coefficients of the FLC in the SmC* phase (58.1°C). To compare, both real and imaginary indices of refraction are also shown. The dashed line indicates possible position of the absorption band.

In Fig. 4, we illustrate the imaginary indices of refraction of the FLC in the SmA* phase, κ_e and κ_o, the absorption coefficients, α_e and α_o, together with the real indices. Corresponding data for the SmC* phase are shown in Fig. 5. The imaginary indices are in general less than 0.06, while the corresponding absorption coefficients of the FLC are found to be less than 5 cm^{-1} below 1 THz. Several broad absorption features can be discerned. The dashed lines in Fig. 4 indicate the absorption peaks at 1.4 THz for e-waves and 1.75 THz for o-waves, which coincide with anomalous dispersion region of the FLC in the SmA* phase, as expected. The same absorption peak for o-wave is also observed in the SmC* phase as indicated by the dashed line in Fig. 5. Further work is in progress for the identification of these absorption features. We note that the data reported beyond 2.5 THz are less accurate due to the signal-to-noise limitation of the THz time-domain spectrometer.

Conclusions

We report THz-band complex refractive indices of a ferroelectric liquid crystal (ZLI-4654-000) measured by THz time-domain Spectroscopy. In the 0.3 to 3.0 THz range, extraordinary and ordinary refractive indices of the FLC in the SmA* phase (67.9 °C) are determined to be $n_e = 1.54 \sim 1.59$, and $n_o = 1.44 \sim 1.52$. For the SmC* phase (58.1°C), we find $n_e = 1.56 \sim 1.64, n_o = 1.44 \sim 1.51$. The birefringence of the FLC is thus between 0.03 and 0.16, depending on the phase and frequency, comparable to its value in the visible, 0.13. The imaginary indices of refraction of both the SmA* and SmC* phases are ≤ 0.06. Several broad absorption features can be discerned, for example, the ones near 1.4 and 1.75 THz in the SmA* phase. These coincide with anomalous dispersion region of the FLC as expected. Further work is in progress for the identification of these absorption features.

The present study indicates that ferroelectric liquid crystals are also potentially useful for device applications in the THz frequency range. Faster response than that of devices based on nematic liquid crystals is expected.

Acknowledgments

This work was supported in part by the PPAEU-II and grant NSC 95-2221-E-009-249 from the National Science Council as well as the ATU program of the Ministry of Education of the Republic of China.

References

1. C. Y. Chen, C. F. Hsieh, Y. F. Lin, R. P. Pan, and C. L. Pan, *Optics Express* **12**, 2625 (2004).
2. R. P. Pan, C. Y. Chen, T. R. Tsai, and C. L. Pan, *Mol. Cryst. Liq. Crystl.* **421**, 157 (2004).
3. C. Y. Chen, T. R. Tsai, C. L. Pan, and R. P. Pan, *Appl. Phys. Lett.* **83**, 4497 (2003).
4. T. R. Tsai, C. Y. Chen, C. L. Pan, R. P. Pan, and X.-C. Zhang,*IEEE Microwave and Wireless Components letters* **14**, 77 (2004).
5. C. F. Hsieh, R. P. Pan, T. T. Tang, H. L. Chen, and C. L. Pan,*Opt. Lett.* **31**, 1112 (2006).
6. H. Y. Wu, C. F. Hsieh, T. T. Tang, R. P. Pan, and C. L. Pan, *IEEE Photonics Technology Letters* **18**, 1488 (2006).
7. C. Y. Chen, C. L. Pan, C. F. Hsieh, Y. F. Lin, and, R. P. Pan, *Appl. Phy. Letts.* **88**, 101107 (2006).
8. J. Kanbe, H. Inoue, A. Mizutome, Y. Hanyuu, K. Katagiri, S. Yoshihara, *Ferroelectrics* **114**, 3 (1991).
9. D. D. Huang, E. P. Pozhidaev, V. G. Chigrinov, H. L. Cheung, Y. L. Ho, H. S. Kwok, *Displays* **25**, 21 (2004).

10. R. Buerkle, K.-H. Schweikert, E. Lueder, S. Breitfelder, F. R. Reichel, *Proceedings of SPIE-Advances in Optical Information Processing VII* **2754**, 154 (1996).
11. D. Mittleman, *Sensing with Terahertz Radiation*, 1st ed. (Springer, New York 2002).
12. T. R. Tsai, C. Y. Chen, C. L. Pan, R. P. Pan, and X.-C. Zhang, *Appl. Opt.* **42**, 2372 (2003).
13. R. P. Pan, T. R. Tsai, C. Y. Chen, and C. L. Pan, *J. Bio. Phys.* **29**, 335 (2003).
14. R. P. Pan, T. R. Tsai, C. Y. Chen, C. H. Wang , and C. L. Pan, *Mol. Cryst. Liq. Crystl.* **409**, 137 (2004).
15. C. Y. Chen, C. F. Hsieh, Y. F. Lin, R. P. Pan, and C. L. Pan, *Opt. Exp.* **12**, 2625 (2004).
16. F. Rutz, T. Hasek, and M. Koch, H. Richter, and U. Ewert, *Appl. Phys. Lett.* **89**, 221911 (2006).
17. M. Oh-e, H. Yokoyama, M. Koeberg, E. Hendry, and M. Bonn, *Opt. Exp,* **14**, 11433 (2006).
18. J. Nishizawa, T. Yamada, T. Sasaki, T. Tanabe, T. Wadayama, T. Tanno, and K. Suto, *Appl. Surf. Sci.* **252**, 4226 (2006).
19. Y. Takanishi, K. Ishikawa, J. Watanabe, H. Takezoe, M. Yamashita, and K. Kawase, *Phys. Rev. E* **71**, 061701 (2005).